International Journal of Applied Engineering Research
ISSN 0973-4562 Volume 10, Number 2 (2015) pp. 2401-2418

http://www.ripublication.com

EVM Based Performance Analysis Of LTE Downlink & Its Real-Time Evaluation Using WARP

[1]Mugelan R K, [2]Thilaga P, [3]Bhagyaveni M A

[1]Research Scholar, [2]Post Graduate Student, [3]Professor
[1,2,3] Department of ECE, College of Engineering Guindy, Anna University, Chennai-25, Tamil Nadu, India
[1]mugelan.r.k@gmail.com, [2]thilaga8892@gmail.com, [3]bhagya@annauniv.edu

Abstract

Long Term Evolution (LTE) is the next major step in mobile radio communications and is introduced in 3rd Generation Partnership Project (3GPP) Release 8. The aim is to enhance the capacity of LTE which meets the requirements of 4G technologies. Multiple input multiple output (MIMO) technique that requires multiple antennas at both transmitter and the receiver is a key technology to meet the peak data rates, low latency and spectral efficient targets of LTE systems. This paper presents a performance evaluation of LTE downlink physical layer according to the latest 3GPP specifications. Particularly, the main features at the LTE physical layer are described and analyzed. LTE uses Orthogonal Frequency Division Multiplexing (OFDM) in downlink. The main concepts of MIMO such as transmit diversity and spatial multiplexing had been done in wireless open access research platform (WARP). Error Vector Magnitude (EVM) and Bit Error Rate (BER) had been analyzed for spatial multiplexing and transmit diversity under different modulation schemes. It is observed that MIMO with Alamouti scheme provides better EVM and BER performance than spatial multiplexing.

Key words: SISO, MIMO, spatial multiplexing, transmit diversity, alamouti, wireless open access research platform.

I. Introduction
Cellular operators are competing traditional broadband operators by offering mobile broadband access and IP services such as rich multimedia (e.g., video-on-demand, music download, video sharing) to laptops, PDAs, smart-phones and other advanced handsets. They offer these services through access networks such as High-Speed

Packet Access (HSPA), Evolution-Data Optimized (EV-DO). The new technologies offers mobile operators significantly improved data speeds, short latency and increased capacity. LTE is the next major step in mobile radio communications. The requirements are high speed data rate, higher spectral efficiency, improved services and lower latency as well as high-capacity voice support. LTE primarily uses the concept of MIMO and OFDM. Multiple input multiple output (MIMO) technique that requires multiple antennas at both transmitter and the receiver is a key technology to meet the targets of LTE. The advantages in MIMO are transmit diversity and spatial multiplexing. Transmit diversity is a technique used to transmit multiple copies of a data stream across a number of antennas and to exploit the various received versions of the data to improve the reliability of data-transfer. Through spatial multiplexing, data rate can be increased where data is divided into separate streams and by transmitting independent information streams in parallel through spatial channels. To achieve improved capacity, transmit diversity and spatial multiplexing are employed. This had been done in wireless research tool called wireless open access research platform (WARP). The basic principle, capacity performance and application scenarios of transmit diversity and spatial multiplexing had been analyzed [1]. Different channel estimation methods such as zero forcing (ZF), minimum mean square error (MMSE) and singular value decomposition (SVD) had been discussed to reduce the time to compute the parameters of time domain channel model and zero forcing is found to be simple [2]. In [3] transmit diversity and spatial multiplexing were discussed and they proposed that both can be done simultaneously but there is a fundamental tradeoff between them. Space time block codes can be used for achieving full diversity gain and to make the transmission reliable [4].

WARP provides a scalable and configurable platform mainly designed to prototype wireless communication algorithms for educational and research oriented applications. In this paper, we analyze performance of MIMO especially spatial multiplexing and STBC under different modulation scheme based on error vector magnitude (EVM). EVM is being calculated from receiver constellation diagram which can be used to assess the quality of digitally modulated signal [5]. Since there exist direct relationship between BER and EVM, it is better to calculate EVM, because EVM is an equivalent performance metric of BER which can be obtained without demodulation and decoding which save considerable time and complexity in the receiver.

The rest of the paper is organized as follows. Section II discusses about the features of WARP kit. In Section III we have discussed about the detailed architecture of SISO-OFDM and MIMO-OFDM links. The system model taken for the real time evaluation has been shown in Section IV. Results and Future work are stated in Section V and VI respectively.

II. WARP

A. Wireless Open Access Research Platform

The WARP platform shown in Figure 2.1, was designed at Rice University and is used by number of academic and industrial research lab for clean state protocol implementation of the MAC and PHY[6]. A WARPV3 node usually contains two RF node (RF A, RF B) which is suitable for SISO transmission, each RF node can be configured as either transmitter or receiver. Two more RF node (RF C, RF D) can be added via FMC (FPGA Mezzanine Connector) for MIMO transmission. Multiple WARP nodes can be connected to same computer via Ethernet switch.

Figure 2.1: WARP FPGA and MIMO-capable radios

Three main component of WARP are (a)XilinxVirtex-II: MAC protocols are written in C and targeted to embedded PowerPC cores whereas PHY protocol are implemented within the FPGA fabric to achieve required parallelization (b)MIMI capable radios: upto four 2.4/5GHz can be configured and can support wideband applications.

B. WARPLab 7

The WARPLab is a framework for rapid prototyping that allows for coordination of arbitrary combination of single and multi-antenna transmit and receive nodes. The extensible framework gives user the flexibility to develop and deploy large array of nodes to meet any application or research need. The WARPLab reference design is an implementation of the WARPLab framework that allows many physical layer designs to be constructed and tested. The reference design combines MATLAB and FPGA implementations of the WARPLab framework modules that allow for easy extensibility and customization. While reference design uses MATLAB to control nodes and perform signal processing, it also allows application with strict latency requirements to move time critical processing in to FPGA.

III. Architecture

A. Single Input and Single Output (SISO System

The Figure 3.1 depicts the various functional blocks of SISO-OFDM link. In SISO, the information bits are generated, complex symbol mapping is done and inverse fast Fourier transform is taken to convert frequency domain signals into OFDM time domain signals. Cyclic prefix is added to overcome interference between subcarriers and parallel to serial conversion takes place and then it is transmitted via single antenna which operates at 2.4GHz.

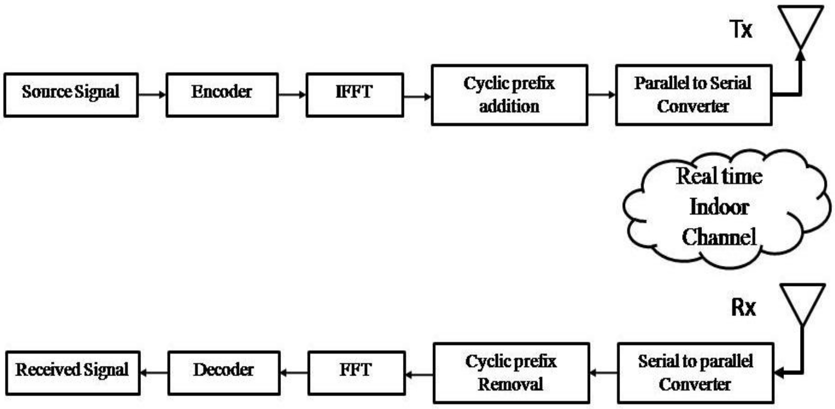

Figure 3.1 SISO-OFDM functional Block diagram

B. Multiple Input and Multiple Output (MIMO) System

In MIMO, the information bits are generated and encoding is done. Information symbols are divided into two data streams and inverse fast Fourier transform, addition of cyclic prefix, parallel to serial conversions are taken separately for two data streams and sent through two antennas. When spatial multiplexing has to be done as shown in Figure 3.2, two different data streams are sent through two antennas. When transmit diversity has to be done as shown in figure 3.2, same data is sent through two antennas. In receiver part, data is received via single antenna in MISO and is received via two antennas in MIMO. In both cases, serial to parallel conversion, removal of cyclic prefix and fast Fourier transform are done in order and finally data is decoded and retrieved.

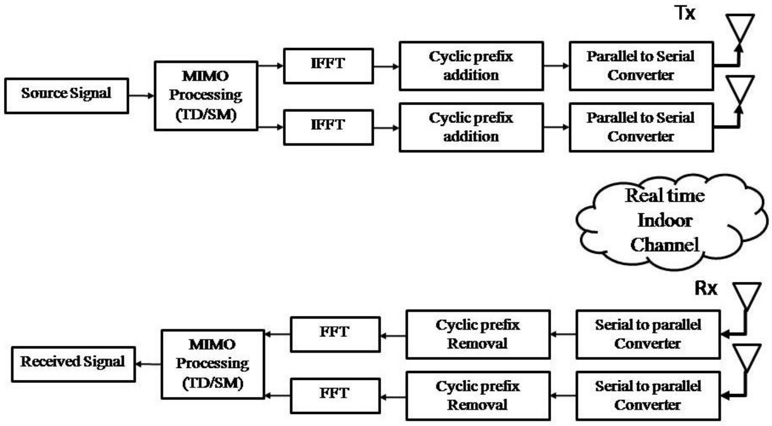

Figure 3.2 MIMO-OFDM (TD/SM) functional Block Diagram

IV. System Model

A. Signal Modelling

By combining both the effects of multipath propagation and fading on a wireless transmission, the received signal baseband equivalent r(t) can be expressed as [7],

$$r(t) = \sum_{i=1}^{N} \rho_i(t) e^{j\theta_i(t)} x[t - \tau_i(t)] + n(t) \quad (1)$$

where x(t) is the transmitted signal baseband equivalent in N number of multipath to the receiver, $\rho_i(t)$ and $\theta_i(t)$ are the time-varying attenuation and phase shift respectively of the i-th path, $\tau_i(t)$ is a function of time and n(t) is a white Gaussian noise. Now equation (1) can be written as,

$$r(t) = \sum_{i=1}^{N} h_i(t) x[t - \tau_i] + n(t) \quad (2)$$

where, $h_i(t) = \rho_i(t) e^{j\theta_i(t)}$ (3)

the equation (2) denotes the received signal in a frequency selective channel.

For real-time indoor channel, the path is a flat fading multipath channel. Hence equation (2) can be modified and depicted as follows,

$$r(t) = \sum_{i=1}^{N} h_i(t) x[\, t - \bar{\tau}\,] + n(t) \quad (4)$$

if N>>1,

$$r(t) = h(t).\, x(t - \bar{\tau}\,) + n(t) \quad (5)$$

$$h(t) = h_R(t) + jh_I(t) \quad (6)$$

B. Channel Modelling

The WARP test bed is used in an indoor environment with probability density function described as [8],

$$P_{real} = \frac{r}{\sigma^2} exp\left(\frac{r^2+c^2}{2\sigma^2}\right) I_0\left(\frac{r^2 c}{\sigma^2}\right) \quad (7)$$

Where, 'c' is the direct component, and 'σ^{2}' is the average power of multipath signal. The field strength of the receiver is described as,

$$\bar{E}_\tau = \sum_\tau \bar{E}_i \quad (8)$$

$$\bar{E}_i = L_i(s) \prod_i \bar{\bar{R}}(\theta_{ij}) \overline{E_0} \quad (9)$$

Where 'i' is the number of propagation path between the transmitter and receiver and 'j' is the number of reflection. $\bar{E}_i$ is the received field strength vector of i th ray in the receiver. $\overline{E_0}$ is the transmit field strength vector of 1m from the transmitter, reference field strength. $L_i(s)$ is path loss of i th ray in the receiver through the path s in the free space. $\bar{\bar{R}}(\theta_{ij})$ is the reflection coefficient of j th reflection of the i th ray, incidence angle is θ_{ij}. For the arrival of one incident ray, we can have three different cases of received field strength as,

Case 1: Direct Ray

$$E_{LOS} = E_0 \frac{e^{-jkd}}{d} \quad (10)$$

Case 2: Reflected Ray

$$E_R = E_0 \bar{R} \frac{e^{-jkd(s+s')}}{(s+s')} \quad (11)$$

Case 3: Diffracted Ray

$$E_D = \frac{E_0}{s'} \bar{D} \sqrt{\frac{s'}{s(s+s')}}\, e^{-jkd(s+s')} \quad (12)$$

Where, 'k' is a propagation constant, E_0 is transmit field strength, 'd' is propagating path length, s' is path length from the source to diffraction edge, s is path length from diffraction edge to the receiver, $\bar{R}$ is the Fresnel reflection coefficient, $\bar{D}$ is diffraction coefficient of the limited conductor edge. If number of rays is j, the total field strength is given by,

$$E_{TOT} = \sum_j E_j \quad (13)$$

And path loss is,

$$L = 20log\left(\frac{\lambda}{4\pi}\frac{E_{TOT}}{E_0}\right) \quad (14)$$

For Indoor channel model, the channel matrix is given by,

$$H = H_d + H_m \quad (15)$$

$$= \sqrt{\frac{K}{K+1}}\, H_{d,n} + \sqrt{\frac{1}{K+1}}\, H_{m,n} \quad (16)$$

where, H_d is the direct and multipath components of the channel matrix respectively. $H_{d,n}$ and $H_{m,n}$ are the normalized values with $\|H_{d,n}\|^2 = N_T N_R$ and $E\left\{\left|[H_{m,n}]_{i,j}\right|^2\right\} = 1$, for i-=1:$N_R$, j= 1:$N_T$. Note that the Rician K-factor is the power ratio of the deterministic and random components of the channel as,

$$K = \frac{\left|[H_{i,j}]\right|^2}{E\left\{\left|[H_{i,j}]\right|^2\right\}} \quad (17)$$

For an indoor channel the value of K ranges from 4<K<12dB, in our experimental setup the rician factor K is, K=7.98dB for transmission power of, P_t= 30dBm and RSSI = -60dB. Hence we conclude that the channel in which, WARP test bed is being operated is a Rician Flat fading Indoor Channel model.

C. Spatial Multiplexing (SM)

MIMO systems offer a linear increase in data rate through spatial multiplexing i.e., transmitting multiple, independent data streams within the bandwidth of operation. In general, the number of data streams that can be reliably supported by a MIMO channel equals the minimum of the number of transmit antennas and the number of receive antennas, i.e., min{MT,MR}. The spatial multiplexing gain increases the capacity of a wireless network.

In figure 4.1 we show how a signal is being transmitted in spatial multiplexing mode and how their performances are being evaluated. Below table 4.1 shows the OFDM parameters.

TABLE 4.1 Experimental Parameters

Parameters	**Values**
Number of OFDM Symbols	10 to 180
Modulation Order	2(BPSK)/4(QPSK)/ 16(16-QAM)
Transmission scale	1.0
Number of Sub-Carriers	64
Cyclic prefix length	16
FFT/IFFT point	64
FFT offset	4
LTS correlation Threshold	0.8
MIMO mode	2x2

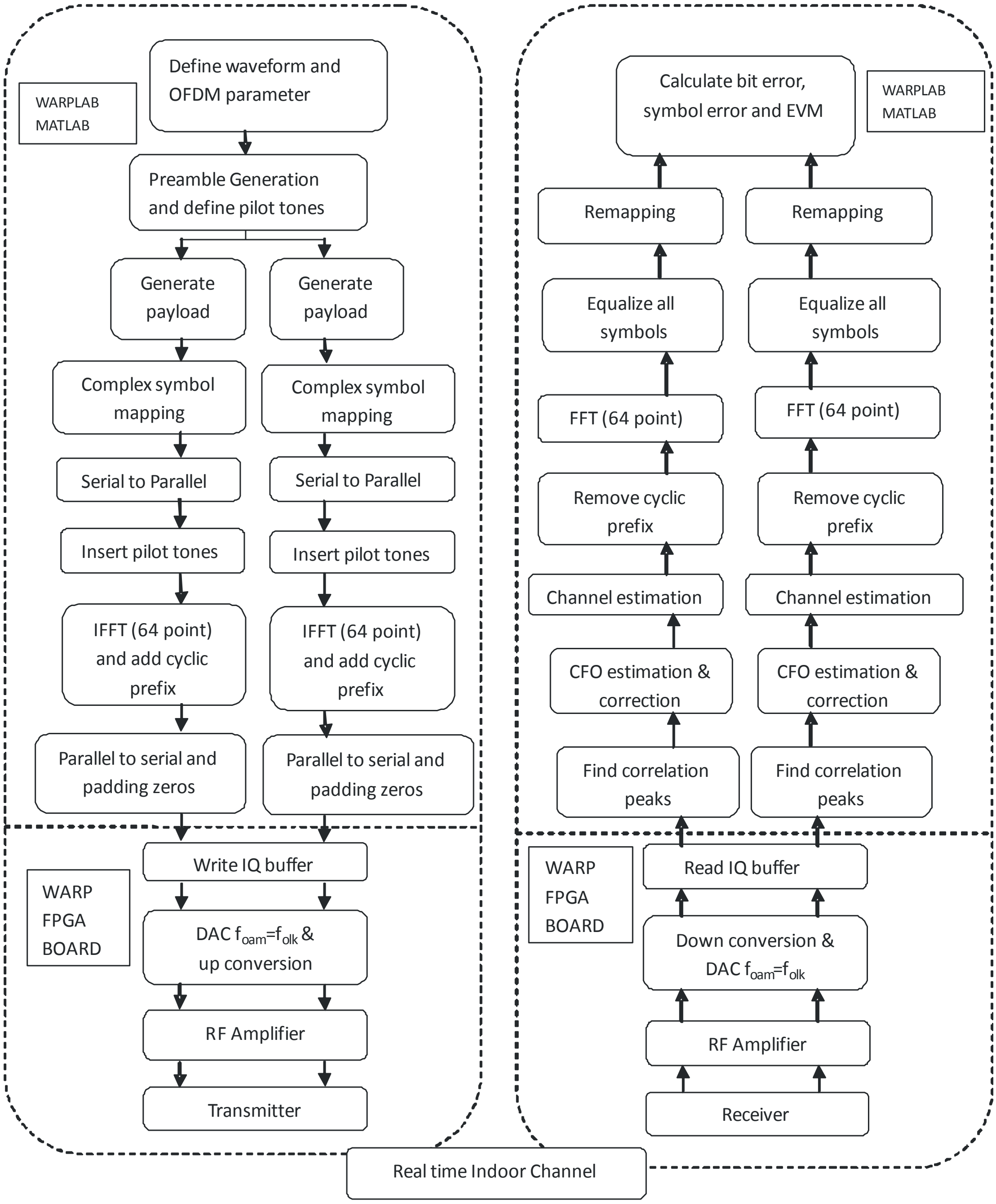

Figure 4.1 Flow Chart of 2x2 Spatial multiplexing implementation in WARP

1.) Transmitter

After setting the parameters we generate preamble sequences as follows, we chose Short training sequence (STS-f) = 64 samples and (STS-t) = 16 samples which is repeated 30 times giving 480 samples. The long training sequence (LTS) = 64 samples repeating 2.5 times giving 160 samples. Altogether we get the entire preamble sequence of length 640 samples (LTS+STS). Now two different transmitting data sequence are being generated randomly with respect to N_{OFDM} number of symbols and N_{DATA} number of data symbols.

The data bits inserted from the source are firstly mapped (BPSK, QPSK, 64-QAM) using chosen modulation techniques and after that converted from serial to parallel through S-P convertor. Pilot tones are defined as [1 1 -1 1] and the pilot sub carrier indices are [8 22 44 58] then these pilot tones are inserted and repeated for every N_{OFDM}

64-point IDFT is applied to the codeword C = [c_0 c_1.....c_{63}] generated to convert it to time domain. IDFT output at n^{th} time interval (n= 0,1,...63)will be given as,

$$x_n = \frac{1}{8}\sum_{k=0}^{63} c_k e^{\frac{j2\pi kn}{64}} \tag{18}$$

In matrix form,

$$[x_0 x_1 \ldots \ldots x_{63}]^T = D^H [c_0 c_1 \ldots \ldots c_{63}]^T \tag{19}$$

$$[x_0^T x_1^T \ldots \ldots x_{63}^T]^T = (D^H \otimes I_2)[c_0^T c_1^T \ldots \ldots c_{63}^T]^T \tag{20}$$

The 64×64 matrix D^H realizes the IDFT operation. Hence D is a DFT matrix.

After converting the codeword into time domain to avoid inter-symbol interference, a guard interval vector (Cyclic Prefix) of length 16 demoted as X_g= $[x_{-16}x_{-15} \ldots \ldots x_1]$ is added in front of the codeword X = $[x_0 x_1 \ldots \ldots x_{63}]$ so that OFDM symbol X'=[X_g X].

After IFFT processing and cyclic prefix addition, the parallel streams are converted into serial time domain samples using multiplexer and making it ready to transmit through air using multiple carrier frequency. Now the data to be transmitted have to be padded with zeros in order to match the buffer size of the WARP kit. The buffer size of each radio board is 32768.

Now the data to be transmitted is given as an input to WARP kit which will be time domain samples with real and imaginary parts. They are stored separately on I & Q buffer. The stored data is converted into analog waveforms using a DAC. Two analog waveforms are generated separately from real valued samples obtained from I & Q. Here f_{sam}=f_{clk}=40 MHz. . Now the baseband signal is upconverted to RF carrier frequency. Then finally the modulated signal is amplified using RF amplifier and transmitted using Tx antenna 1 and Tx antenna 2.

2.) Receiver

RF signal is received by Rx antenna 1 and Rx antenna 1 which will be amplified using power amplifier to increase its signal strength and then down converted into baseband frequency. The incoming signal is correlated with inphase and quadrature carrier separately to recover inphase and quadrature baseband component separately. Further the analog waveform is converted into digital samples using ADC. The sampling frequency of ADC is equal to buffer clock frequency. Inphase and

Quadrature samples are obtained from separate ADC. After ADC conversion samples are stored in Buffer. As the samples are not passed through FFT block now the samples are in time domain. So received time domain LTS samples are correlated with received vector samples.

LTS= 64 Samples.

In time domain OFDM waveform involves repeated block of [LTS STS Payload]. As LTS is transmitted by both antenna and by performing correlation of them it gives two peaks and doing autocorrelation gives peak in the middle. The difference between two peaks gives timing information about one OFDM symbol because number of samples in LTS and OFDM symbol are equal.

In a communication system, Carrier Frequency Offset (CFO) refers to the difference in carrier frequency at transmitter and receiver. This offset is termed as CFO. The input carrier frequency at the receiver can vary due to Doppler Effect, caused by relative motion between Tx and Rx and is another source of CFO. the frequency offset value is determined as,

$$r(t) = x(t)e^{j2\pi f_\Delta t} \tag{21}$$

Given that short preamble is periodic with $\delta_t = 0.8\ \mu s$

$$r(t-\delta t) = x(t)e^{j2\pi f_\Delta (t-\delta t)} \tag{22}$$

At the receiver as both $x(t)$ and $r(t)$ are known, taking angle of both sides of the equation (22) we get the frequency offset as,

$$\Delta_f = -\frac{\forall y(t-\delta t)y^*(t)}{2\pi\delta t} \tag{23}$$

The LTS samples which are not CFO corrected are extracted. After estimating the carrier frequency offset value, each samples are corrected with the offset value.

Then comes the process of channel estimation, to reduce the computation complexity here we have considered Zero-Forcing technique for estimating the channel. For a perfect CSI, the ZF detection weight matrix W is given by the pseudo-inverse of the channel matrix H, i.e.,

$$W = (H^H H)^{-1} H^H \tag{24}$$

At the receiver, the guard interval is first removed and 64 output samples are gathered from the received signal as,

$$[r_0^T r_1^T \dots \dots r_{63}^T]^T = H_g[x_{-16}^T x_{-15}^T \dots x_{-1}^T\ x_0^T \dots x_{63}^T]^T + [n_0^T n_1^T \dots \dots n_{63}^T]^T \tag{25}$$

where H_g is 128x158 ($64n_r$ x $n_{ot}(64+16-1)$) matrix representing the channel seen by the OFDM symbol.

The system model of equation (25) can be rewritten as,

$$[r_0^T r_1^T \dots \dots r_{63}^T]^T = H_{cp}[\, x_0^T \dots x_{63}^T]^T + \, [n_0^T n_1^T \dots \dots n_{63}^T]^T \tag{26}$$

where H_{cp} is a block wise circulate matrix of size 128x128 matrix. As a result, its SVD decomposition $H_{cp} = (\mathrm{D^H} \otimes \mathrm{I}_2)\mathrm{D_{cp}}(\mathrm{D} \otimes \mathrm{I}_2)$ is such that D_{cp} is a block diagonal matrix whose blocks are obtained by a block wise FFT. The full information about the channel is accounted for in D_{ip}, and the eigenvectors of H_{ip} are independent of the channel matrix H. So equation (26) can be written as,

$$[r_0^T r_1^T \dots \dots r_{63}^T]^T = (D^H \otimes I_2)D_{cp}[\, c_0^T \dots c_{63}^T]^T + \, [n_0^T n_1^T \dots \dots n_{63}^T]^T \tag{27}$$

Applying a 64-FFT operation to the received vector, we finally obtain

$$R = r_k = \sqrt{E_s} H_{(k)} c_k + n_k = XH + N \tag{28}$$

Then, the ZF symbol vector estimate, $\hat{X}$ is

$$\hat{X} = WR = (H^H H)^{-1} H^H \, X + (H^H H)^{-1} H^H N = X + (H^H H)^{-1} H^H N \tag{28}$$

i.e., ZF detection attempts to eliminate the inter-stream interference.

Given the estimate $\hat{H}$ of H, ZF detection estimates the symbol transmitted through the k[th] antenna by mapping the k[th] element of the two dimensional vector, into the closest modulation constellation symbol.

$$\hat{W} R = \left[\hat{H}^H \hat{H}\right]^{-1} + \hat{H}^H X + \left[\hat{H}^H \hat{H}\right]^{-1} \hat{H}^H N \tag{29}$$

D. Transmit Diversity (Alamouti Scheme)

Transmit diversity is desirable in systems where more space, power, and processing capability are available on the transmit side than on the receive side. Transmit diversity design depends on whether or not the complex channel gain is known to the transmitter. When this gain is known, the system is quite similar to receiver diversity. However, without this channel knowledge, transmit diversity gain requires a combination of space and time diversity via a novel technique called the Alamouti scheme [9].

Here a single data stream is divided in two and fed to two transmitting antenna. Consider that two symbols $s_1$and s_2 are transmitted simultaneously from transmit antennas 1 and 2 during the first symbol period, while symbols$-s_2^*$ and s_1^* are transmitted from antennas 1 and 2 during the next symbol period. Assume that the flat fading channel remains constant over the two successive symbol periods, and that the 2×2 channel matrix reads as,

$$H = \begin{bmatrix} h_{11} & h_{12} \\ h_{21} & h_{22} \end{bmatrix} \tag{30}$$

The vector signal received at the receive array at the first symbol period is,

$$r_1 = \sqrt{E_s} H \begin{bmatrix} s_1/\sqrt{2} \\ s_2/\sqrt{2} \end{bmatrix} + n_1 \tag{31}$$

And the vector signal received at the second symbol period is

$$r_2 = \sqrt{E_s} H \begin{bmatrix} -s_2^*/\sqrt{2} \\ s_1^*/\sqrt{2} \end{bmatrix} + n_1 \tag{32}$$

Where n_1 and n_2 are the additive noise contributions at each symbol period over the receive antenna array. The receiver forms a combined signal vector as,

$$r = \begin{bmatrix} r_1 \\ r_2^* \end{bmatrix} = \sqrt{E_s} \underbrace{\begin{bmatrix} h_{11} & h_{12} \\ h_{21} & h_{22} \\ h_{12}^* & -h_{11}^* \\ h_{22}^* & -h_{21}^* \end{bmatrix}}_{\boldsymbol{H_{eff}}} \underbrace{\begin{bmatrix} s_1/\sqrt{2} \\ s_2/\sqrt{2} \end{bmatrix}}_{\boldsymbol{s}} + \begin{bmatrix} n_1 \\ n_2^* \end{bmatrix} \tag{33}$$

Both symbols s_1 and s_2 are spread over the two transmit antennas and over the two symbol periods. Furthermore, H_{eff} is orthogonal for all channel realizations i.e., $H_{eff}^H H_{eff} = \|H\|_F^2 I_2$. If we compute $z = H_{eff}^H y$, we get

$$z = \begin{bmatrix} z_1 \\ z_2 \end{bmatrix} = \sqrt{E_s} H_{eff}^H r = \|H\|_F^2 I_2 s + n', \tag{34}$$

where n' is such that $\varepsilon\{n'\} = 0_{2x1}$ and $\varepsilon\{n' n'^H\} = \|H\|_F^2 \sigma_n^2 I_2$. The above equation illustrates that the transmission of s_1 and s_2 is fully decoupled [10], i.e.,

$$z_k = \sqrt{E_s/2}\, \|H\|_F^2 s_k + \widehat{n_k} \tag{35}$$

k=1,2

The figure 4.1 can be modified as shown in figure 4.2 to show the exact position of alamouti encoder and decoder in the MIMO-OFDM link to obtain a transmit diversity. The rest of the blocks perform the same operation as spatial multiplexing.

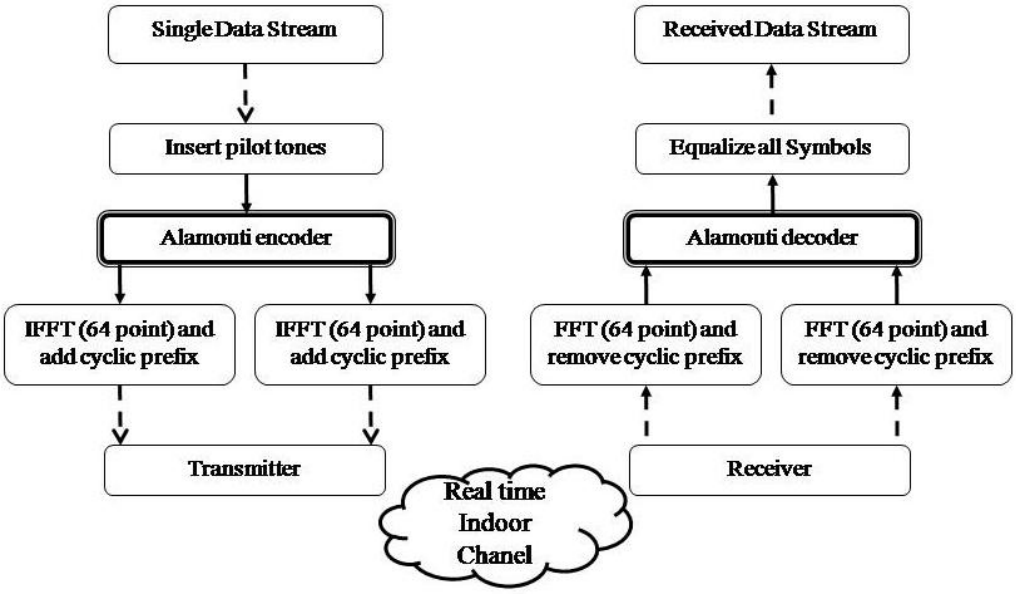

Figure 4.2 Flow chart for 2x2 Transmit diversity using Alamouti scheme in WARP

V. Results And Discussions

After receiving the symbols, error vector magnitude is being found to assess the quality of received signal. Error Vector Magnitude is the vector difference between transmitted signal (ideal symbol) and received signal (measured symbol). EVM helps in identifying sources of signal degradation i.e., phase noise, I-Q imbalance, amplitude non-linearity and filter distortion. Error Vector Magnitude can be expressed as [11] ,

$$EVM = \sqrt{\frac{\frac{1}{N}\sum_{K=1}^{N}(e_K)}{\frac{1}{N}\sum_{K=1}^{N}(I_K^2 + Q_K^2)}} \qquad (36)$$

$$e_K = (I_K - \widetilde{I_k})^2 + (Q_K - \widetilde{Q_k})^2 \qquad (37)$$

Where I_k and Q_k are ideal values (transmitted symbols)
$\widetilde{I_k}$ and $\widetilde{Q_k}$ are received symbols
I_k is the inphase measurement of the k^{th} symbol in the burst
Q_k is the quadrature phase measurement of the k^{th} symbol in the burst
N is the input vector length

Energy consumption for EVM evaluation & SNR evaluation is given by,

$$E_{EVM} = f\{N_{Data\_sym} * E_s\} \qquad (38)$$

$$E_{SNR} = f\{N_{Data\_bit} * E_b\} \quad (39)$$

Where N_{Data_sym} -Number of data symbols, N_{Data_bit}- Number of Data bits, E_s- energy per symbol and E_b- energy per data bit.

The relation between energy per symbol and energy per data bit for M order modulation scheme is given by,

$$E_s = log_2 M E_b \quad (40)$$

The table 5.1 shows the number of data bits N_{Data_bit} required for number of data symbols N_{Data_sym} using various modulation M techniques,

TABLE 4.1 Comparisons between N_{Data_sym} and N_{Data_bit}

N_{Data_sym}	N_{Data_bit}		
	BPSK	**QPSK**	**16-QAM**
960	960	1920	3840
1920	1920	3840	7680
2880	2880	5760	11520
3840	3840	7680	15360
4800	4800	9600	19200
5760	5760	11520	23040
6720	6720	13440	26880
7680	7680	15360	30720
8640	8640	17280	34560

From the figure 5.1, performance of SISO for various modulation schemes has been analyzed. It is observed that, when the numbers of OFDM symbols are increased, error vector magnitude increases and also EVM increases for higher modulation order.

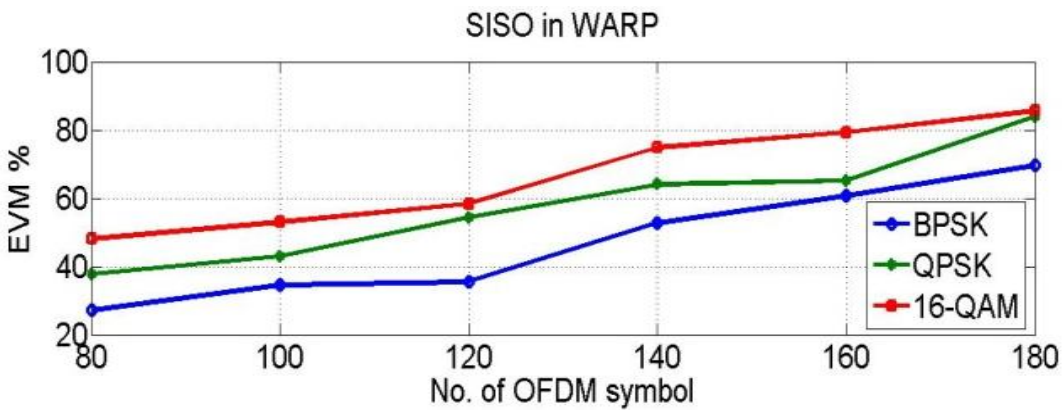

Figure 5.1 OFDM symbols Vs EVM for SISO in WARP

The comparison graph between spatial multiplexing and transmit diversity with Alamouti scheme had been shown in figure 5.2. The graph is for number of OFDM symbol Vs EVM. It had been analyzed for 16-QAM modulation scheme. Alamouti scheme gives better performance than spatial multiplexing.

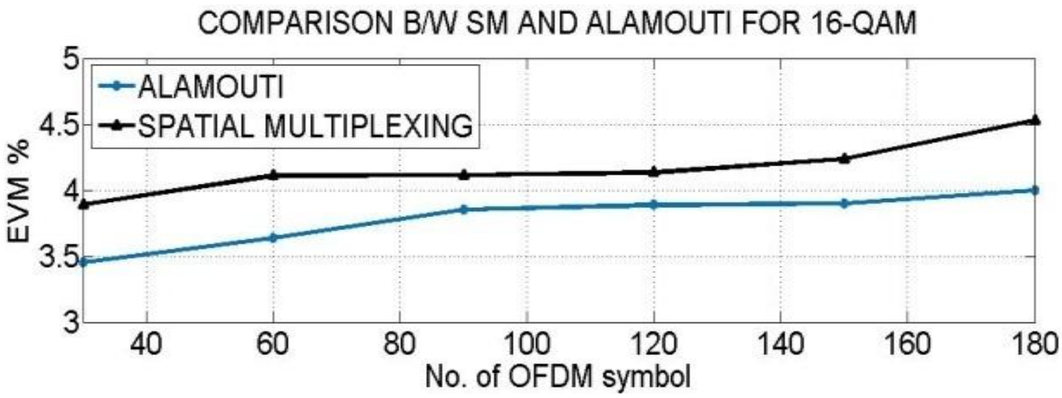

Figure 5.2 Comparison between Spatial multiplexing and Transmit diversity with Alamouti scheme

The figure 5.3 shows the comparison between SISO, spatial multiplexing and transmit diversity with Alamouti scheme for transmitter gain Vs BER. It had been analyzed for 16-QAM modulation scheme with 180 OFDM symbols. Alamouti scheme gives better result compared to all but for the range of transmitter gain of 5 to 10 dBm.

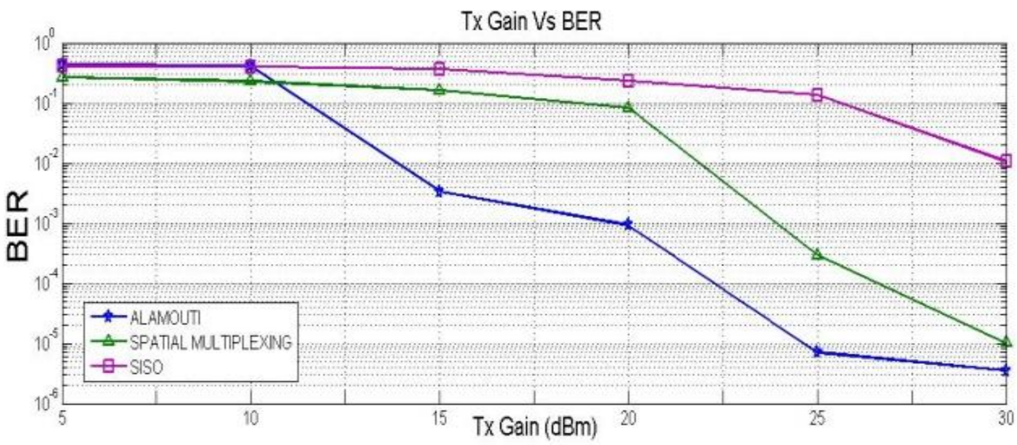

Figure 5.3 Tx gain Vs BER for SISO, SM and TD

From the figure 5.4, it is observed that when the distance between transmit and receive antenna increases, BER increases in all cases i.e., SISO, spatial multiplexing and Alamouti scheme. It had been analyzed for 16-QAM modulation scheme with 180 OFDM symbols. For applications with less data rate whose requested BER are less than 10^{-3}, SISO will be suitable. e.g., for WSN using light application such as temperature sensing, BER will be less than 10^{-3}. In that case SISO will be advantageous upto 2 feet (0.6096m). For above 2 feet, SISO gives BER of 10^{-2} which won't be useful. For 1 foot (0.3048m), spatial multiplexing gives BER of 10^{-5} and Alamouti gives BER of 10^{-7}.

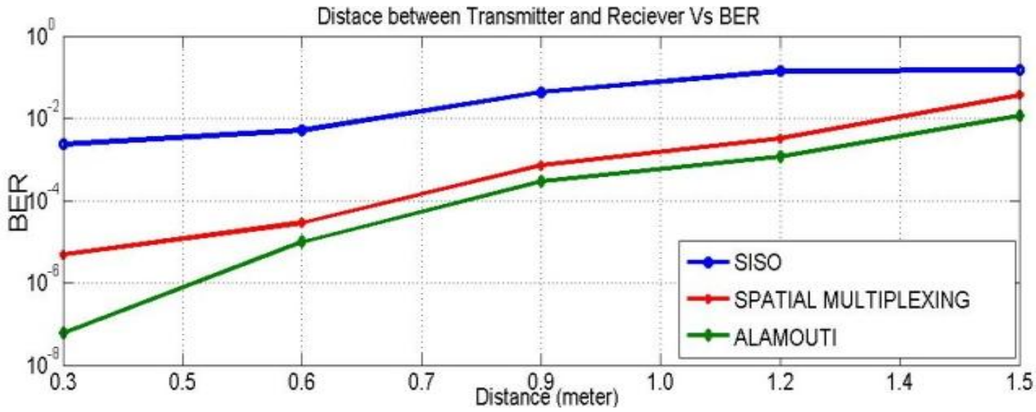

Figure 5.4 Distance between Tx and Rx Vs BER

VI. Future Work

The future work is to adaptively harvest the advantages of both spatial multiplexing and Transmit diversity by adaptively switching the antennas between these two modes based on various parameter such as data rate, BER, etc.,

VII. References

[1] Wei Liu, Kaikai Liu, Nan Li, Jiangbo Dong, Na Liu, Yanlei Chen,Hao Sun, and Yunbo Han, "Investigation of adaptive multi-antenna switching strategy in TD-LTE systems", Progress In Electromagnetics Research Symposium Proceedings, Moscow, pages:1579-1583, 2012.

[2] Wang Hong-jin, Liu Li-fa, "A modified channel estimation based on SVD in LTE-Advanced systems", IEEE conference publications, pages: 492-497, 2011.

[3] Zhang, L. Z. and D. N. C. Tse, "Diversity and multiplexing: A fundamental tradeoff in multiple antenna channels", IEEE Transactions on Information Theory, Vol. 49, No. 5, pages:1073-1096, 2003.

[4] V. Tarokh, H. Jafarkhani, and A. R. Calderbank, "Space-time block code from orthogonal designs", IEEE Transactions on Information Theory, Vol. 45, pages:1456–1467, July 1999.

[5] Rishad Ahmed Shafik, Md. Shahriar Rahman, AHM Razibul Islam and Nabil Shovon Ashraf. "The Error Vector Magnitude as a performance metric and

comparative analysis", IEEE-ICET, 2nd International Conference on Emerging Technologies Peshawar, Pakistan, pages: 13-14, November 2006.

[6] P. Murphy, A. Sabharwal, and B. Aazhang. Design of WARP: Wireless open-access research platform. In *European Signal Processing Conference,* June 2006.

[7] Antonio Petrolino, Gonçalo Tavares," Simulation of SISO and MIMO Multipath Fading Channels", INESC-ID www.intechopen.com.

[8] Jianpei Chen et.al, "Physical Statistical Modelling of Mimo Channel Based on Rician Distribution", Global Mobile Congress (GMC), pp 1-7, 2011.

[9] Andrea Goldsmith, "Wireless Communications", Cambridge University Press, Stanford University, 1st edition, 2005.

[10] Bruno Clerckx, Claude Oestges," MIMO Wireless Networks Channels, Techniques and Standards for Multi-Antenna, Multi-User and Multi-Cell Systems", Elsevier publication, second edition, 2013.

[11] Rishad Ahmed Shafik, Md. Shahriar Rahman, AHM Razibul Islam," On the Extended Relationships Among EVM, BER and SNR as Performance Metrics", 4th International Conference on Electrical and Computer Engineering ICECE 2006, 19-21 December 2006, Dhaka, Bangladesh.

Acknowledgement

We would like to thank Department of Science and Technology, Government of India for supporting the work under the scheme of "FAST TRACK SCHEME FOR YOUNG SCIENTIST" under the grant number SR/FTP/ETA-92/2011.

Biography

Mr. R.K. Mugelan is a Research scholar at the Department of Electronics and Communication Engineering, College of Engineering Guindy, Anna University ,Chennai, Tamil Nadu, India. He completed his B.Tech from, Rajiv Gandhi College of Engineering and Technology, Pondicherry, affiliated to Pondicherry University, India, M.E from College of Engineering Guindy, Anna University ,Chennai India. His field of interests includes Wireless communication and networks, Sensor networks. His current research interests are in the field of Green Communication Networks.

Ms. P. Thilaga is a M.E. Post Graduate student at the Department of Electronics and Communication Engineering, College of Engineering Guindy, Anna University, Chennai, India. She pursued her B.E in Electronics and Communication Engineering from Alagappa Chettiar College of Engineering and Technology, Karaikudi, Tamil Nadu, India. Her field of interest is wireless communication and networks.

Dr. M.A. Bhagyaveni received her B.E. degree in Electronics and Communication Engineering from GCT, Coimbatore, India and M.E. degree in Optical Communication from CEG, Gunidy, India and Ph.D. degree from CEG, Guindy, India . She is currently working as Professor in the Department of Electronics and Communication Engineering, CEG Campus, Anna University, Chennai, India. Her present research interests include Wireless communication, Digital communication, MIMO systems, Ad hoc networks, Sensor networks, Cloud computing, Cognitive radio technologies. She has published more than 20 papers in National/International Journals and Conferences.